

FULL-WAVE SEMICONDUCTOR DEVICES SIMULATION USING ADI-FDTD METHOD

R. Mirzavand[†], A. Abdipour, and G. Moradi

Electrical Engineering Department
Amirkabir University
Tehran 15914, Iran

M. Movahhedi

Electrical Engineering Department
Shahid Bahonar University of Kerman
Kerman, Iran

Abstract—This paper describes the alternating-direction implicit finite-difference time-domain (ADI-FDTD) method for physical modeling of high-frequency semiconductor devices. The model contains the semiconductor equations in conjunction with the Maxwell's equations which describe the complete behavior of high-frequency active devices. Using ADI approach leads to a significant reduction of the full-wave simulation time. We can reach over 99% reduction in the simulation time by using this technique while still have a good degree of accuracy compared to the conventional approaches. As the first step in the performance investigation, we use the electrons flow equations in the absence of holes and recombination as semiconductor equations in this paper.

1. INTRODUCTION

By increasing the operating frequency, devices and circuits need more and more accurate techniques for modeling and simulation [1–3]. If non-local and hot carrier transport of transistors cannot be ignored, the simulation requires more accurate model for semiconductor devices. Many different approaches to the simulation of these devices have

Corresponding author: R. Mirzavand (R.Mirzavand.Boroujeni@tue.nl).

[†] Also with CASA, Technische Universiteit Eindhoven, HG 8.10, P. O. Box 513, 5600 MB, Eindhoven, The Netherlands.

been developed in the past [3–7]. These techniques are fundamentally dependent upon the solution of the Poisson equation along with the basic carrier transport equations. In this paper, the semiconductor analysis is based on the time-domain drift-diffusion method (DDM) [4] in conjunction with Maxwell's equations. The set of DDM equations contains the Poisson equation and the carrier transport equations, obtained by splitting the Boltzmann transport equation (BTE) into its first two moments. The DDM model assumes that the carrier temperature is equal to the semiconductor lattice temperature. Therefore, the carrier velocity is dependent on the electric field only. In comparison to other more rigorous techniques for numerical modeling of semiconductor devices, the DDM is a relatively simple technique with better convergence of the algorithm and shorter computational time. Therefore, it is more suitable for use by a design engineer. On the other hand, even for simple semiconductor equations, the simultaneous simulation of these equations and Maxwell's equations is very time consuming because of the limitations on the simulation time-step. In the last decade, a new method, called the alternating-direction implicit FDTD (ADI-FDTD) method, has been introduced [8, 9] to solve the Maxwell's curl equations. This method is an attractive alternative to the standard FDTD due to its unconditional stability with moderate computational overhead. The unconditional stability means that the ADI-FDTD method is free of the Courant-Friedrich-Levy (CFL) stability restraint, allowing any choice of Δt for a stable solution [10, 11]. The ADI-FDTD can be particularly useful for problems involving devices with fine geometric features that are much smaller than the wavelengths of interest [12–17]. It is used in the semiconductor device simulation for only the electromagnetic model part (Half-ADI scheme). This paper presents an implicit numerical method to solve the DDM and Maxwell's equations based on ADI-FDTD method (Full-ADI scheme). This allows using a larger time-step size that leads significant CPU time reduction in an acceptable degree of accuracy.

2. ACTIVE DEVICE MODEL

The active device model used for simulation is based on the moments of Boltzmann's transport equations obtained by integration over the momentum space. Three equations need to be solved together with Poisson's equation in order to get the quasi-static characteristics of the transistor. This system of coupled highly nonlinear partial differential equations contains current continuity, energy conservation and momentum conservation equations [4]. The solution of this system

of partial differential equations represents the complete hydrodynamic model. Simplified models are obtained neglecting some terms in momentum equation. One of these simplified models is drift-diffusion model (DDM). In this paper we simulate MESFET as microwave/mm transistor that is a unipolar device. For this device, the equations to be solved in the drift-diffusion model are:

$$\nabla^2 \phi = -\frac{\rho}{\varepsilon} = -\frac{q}{\varepsilon_0 \varepsilon_r} (N_d^+ - n), \quad (1)$$

$$\frac{\partial n}{\partial t} = \frac{1}{q} \nabla \cdot \vec{J}_n = \frac{1}{q} \left(\frac{\partial J_x}{\partial x} + \frac{\partial J_y}{\partial y} \right), \quad (2)$$

$$\vec{J}_n = q \cdot n \cdot \mu_n(\vec{E}, N_d) \cdot \vec{E} + q \cdot D_n(\vec{E}, N_d) \cdot \nabla n, \quad (3)$$

$$\vec{E} = -\nabla \phi. \quad (4)$$

where $D_n = \mu_n K_B T / q$, $\mu_n(E, N_d) = [\mu_0 + (v_s/E)(E/E_s)^4] / [1 + (E/E_s)^4]$ have been defined in [18]. In the above equations, ϕ is the potential, N_d is the doping profile, n is the electron concentration, and μ_n and D_n are the mobility and the diffusion coefficient, respectively. Equation (1) can be discretized using the carrier concentration $n_{i,j}$ at $t = k$ as follows:

$$\begin{aligned} & (\phi_{i+1,j} - 2\phi_{i,j} + \phi_{i-1,j}) / (\Delta x^2) + (\phi_{i,j+1} - 2\phi_{i,j} + \phi_{i,j-1}) / (\Delta y^2) \\ & = -q(N_d^+ - n_{i,j}^k) / \varepsilon. \end{aligned} \quad (5)$$

To obtain an unconditionally stable solution, the ADI principle [19] is applied to Equation (2) as follows. The computation of Equation (2) for the FDTD solution marching from the n th time-step to the $(n+1)$ th time-step is broken up into two computational sub-advancements: the advancement from the n th time-step to the $(n+1/2)$ th time-step and the advancement from the $(n+1/2)$ th time-step to the $(n+1)$ th time-step. More specifically, the two substeps are as follows.

Step 1): For the first half-step, i.e., at the $(n+1/2)$ th time step, the first partial derivative on the right-hand side (RHS) of Equation (2), $\partial J_x / \partial x$, is replaced with an implicit difference approximation of its unknown pivotal values at the $(n+1/2)$ th time step, while the second partial derivatives on the RHS, $\partial J_y / \partial y$, is replaced with an explicit FD approximation in its known values at the previous n th time step. Using the first-order upwind scheme for spatial derivatives,

$$v_i \frac{d}{dx} [f_i] = \begin{cases} v_i (f_i - f_{i-1}) / \Delta x & \text{if } v_i \geq 0, \\ v_i (f_{i+1} - f_i) / \Delta x & \text{if } v_i < 0. \end{cases} \quad (6)$$

yields the following equation,

$$\begin{aligned}
& - \left(\frac{dt}{2dx^2} D_{ij} + \frac{dt}{2dx} \mu_{ij} \frac{|E_x| + E_x}{2} \right) n_{i+1,j}^{k+1/2} \\
& + \left(1 + \frac{dt}{dx^2} D_{ij} + \frac{dt}{2dx} \mu_{ij} |E_x| + \frac{dt}{2} \mu_{ij} \nabla^2 \phi \right) n_{i,j}^{k+1/2} \\
& - \left(1 + \frac{dt}{dx^2} D_{ij} + \frac{dt}{2dx} \mu_{ij} |E_x| + \frac{dt}{2} \mu_{ij} \nabla^2 \phi \right) n_{i-1,j}^{k+1/2} \\
= & \left(\frac{dt}{2dy^2} D_{ij} + \frac{dt}{2dy} \mu_{ij} \frac{|E_y| + E_y}{2} \right) n_{i,j+1}^k \\
& + \left(1 - \frac{dt}{dy^2} D_{ij} - \frac{dt}{2dy} \mu_{ij} |E_y| \right) n_{i,j}^k \\
& + \left(\frac{dt}{2dy^2} D_{ij} + \frac{dt}{2dy} \mu_{ij} \frac{|E_y| - E_y}{2} \right) n_{i,j-1}^k. \tag{7}
\end{aligned}$$

Step 2): For the second half time-step, i.e., at $(n+1)$ th time step, the second term on the RHS, $J_y/\partial y$, is replaced with an implicit FD approximation of its unknown pivotal values at the $(n+1)$ th time step, while the first term is replaced with an explicit FD approximation in its known values at the previous $(n+1/2)$ th time-step. Using the first-order upwind scheme for spatial derivatives, the following equation can be derived,

$$\begin{aligned}
& - \left(\frac{dt}{2dy^2} D_{ij} + \frac{dt}{2dy} \mu_{ij} \frac{|E_y| + E_y}{2} \right) n_{i,j+1}^{k+1} \\
& + \left(1 + \frac{dt}{dy^2} D_{ij} + \frac{dt}{2dy} \mu_{ij} |E_y| + \frac{dt}{2} \mu_{ij} \nabla^2 \phi \right) n_{i,j}^{k+1} \\
& - \left(\frac{dt}{2dy^2} D_{ij} + \frac{dt}{2dy} \mu_{ij} \frac{|E_y| - E_y}{2} \right) n_{i,j-1}^{k+1} \\
= & \left(\frac{dt}{2dx^2} D_{ij} + \frac{dt}{2dx} \mu_{ij} \frac{|E_x| + E_x}{2} \right) n_{i+1,j}^{k+1/2} \\
& + \left(1 - \frac{dt}{dx^2} D_{ij} - \frac{dt}{2dx} \mu_{ij} |E_x| \right) n_{i,j}^{k+1/2} \\
& + \left(\frac{dt}{2dx^2} D_{ij} + \frac{dt}{2dx} \mu_{ij} \frac{|E_x| - E_x}{2} \right) n_{i-1,j}^{k+1/2}. \tag{8}
\end{aligned}$$

3. ELECTROMAGNETIC MODEL

The Maxwell's equations characterize electromagnetic wave propagation completely which can be written in a matrix form as

$$D_t W = (D_1 + D_2)W + J. \tag{9}$$

where

$$D_\alpha = \frac{\partial}{\partial \alpha}, \quad W = [E_x \quad E_y \quad E_z \quad H_x \quad H_y \quad H_z],$$

$$J = [J_x \quad J_y \quad J_z \quad 0 \quad 0 \quad 0],$$

$$D_1 = \begin{bmatrix} 0 & 0 & 0 & 0 & -a_1 D_z & 0 \\ 0 & 0 & 0 & 0 & 0 & -a_1 D_x \\ 0 & 0 & 0 & -a_1 D_y & 0 & 0 \\ 0 & 0 & -a_2 D_y & 0 & 0 & 0 \\ -a_2 D_z & 0 & 0 & 0 & 0 & 0 \\ 0 & -a_2 D_x & 0 & 0 & 0 & 0 \end{bmatrix},$$

$$D_2 = \begin{bmatrix} 0 & 0 & 0 & 0 & 0 & a_1 D_y \\ 0 & 0 & 0 & a_1 D_z & 0 & 0 \\ 0 & 0 & 0 & 0 & a_1 D_x & 0 \\ 0 & a_2 D_z & 0 & 0 & 0 & 0 \\ 0 & 0 & a_2 D_y & 0 & 0 & 0 \\ a_2 D_y & 0 & 0 & 0 & 0 & 0 \end{bmatrix}.$$

where \vec{E} is the electric field, \vec{H} is the magnetic field, \vec{D} is the electric flux density, and \vec{B} is the magnetic flux density. To solve Equation (9), algorithm of ADI-FDTD introduced by Namiki [8] and Zheng et al. [9] to eliminate the constraints of the CFL condition in standard FDTD. To solve Equation (9), it is broken up into two time steps at $n + 1/2$ and $n + 1$ as

$$(I - D_1)W^{n+1/2} = (I + D_2)W^n + 0.5J^n, \tag{10}$$

$$(I - D_2)W^{n+1} = (I + D_1)W^{n+1/2} + 0.5J^{n+1/2}. \tag{11}$$

where J is the current density estimate by (3).

4. COMPUTATIONAL PROCEDURE

The coupling between the two models is established by properly transforming the physical parameters (e.g., fields and current densities) from one model to the other. In each time step, the Maxwell's and semiconductor equations should be solved sequentially. First, the Maxwell's equations are solved for the electric and magnetic field distributions using the current density obtained in the previous time

step. Then, the obtained EM fields are used in the semiconductor equations to find the new current density. This process is repeated for each time interval [3, 12]. The full-wave analysis procedure includes the following.

1) *Steady-State DC Solution (Initialization)*: The steady-state dc solution for electric fields, current densities, and the other transport parameters are obtained from the semiconductor model by solving Poisson's and hydrodynamic transport equations. The device is biased and the dc parameter distributions (E , n , ϕ , and J_{dc}) are obtained by solving the equations (3)–(5) and (7)–(8), as shown in Figure 1(a). The system of linear equations (7)–(8) are symmetric and tridiagonal, and thus cheap to solve by methods like Choleski decomposition [20]. These dc solutions serve as the corresponding initial values inside the AD for the coupled model.

2) *Time-Domain AC Solution*: After completing the initializations, the AC excitation is applied ($J = J_{dc} + J_{ac}$). The time-domain distribution of the EM fields is obtained using Maxwell's equations. These EM fields are used by the semiconductor model to update the current density. More details about AC and DC solutions can be found in [3]. Figure 1 shows flowchart of the sequence of ADI-FDTD schemes

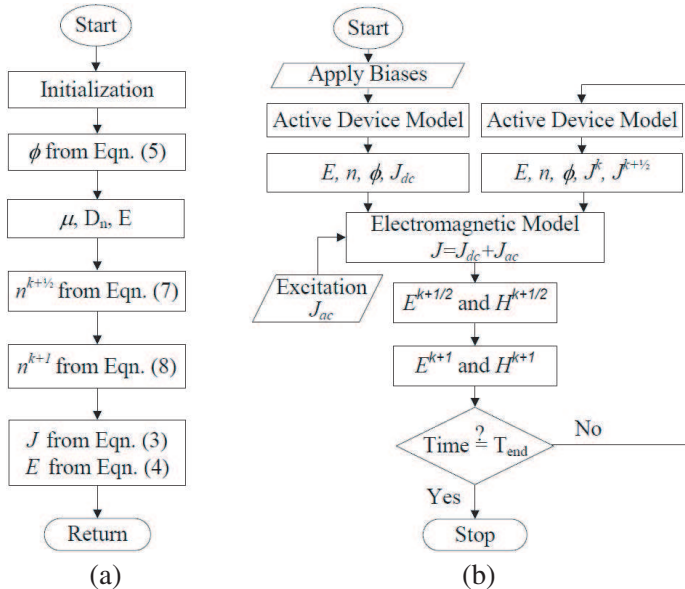


Figure 1. Flowcharts of the sequence of (a) ADI-FDTD scheme for active device model, (b) Full-wave simulation of a semiconductor device.

for full-wave simulation of a semiconductor device contains active device and electromagnetic models.

5. SIMULATION RESULTS

In order to demonstrate the performance of the proposed approach, first the GaAs MESFET transistor shown in Figure 2 is considered. This transistor has an EMS excitation with $f_{\max} = 100$ GHz, large applied electric field, and heavily doped $N_d = 2 \times 10^{17}$ cm⁻³. Because two equation systems must be solved simultaneously, the cell size is chosen equal to 0.01 μm for x and y directions [3] and 1 μm for z direction. For the given cell size, the time-step must be chosen less than 0.01 fs [3]. If the ADI-FDTD method is used to solve the electromagnetic model (Half-ADI scheme), the time-step limit increases from 0.01 fs to 1 fs [12]. The new limitation is because the time-step size in the explicit methods for the semiconductor equations is a function of the average carrier velocity v_d and the spatial step to comply with the following CFL condition for stability and minimizing numerical dispersion [21]:

$$v_d \Delta t \leq [\Delta x^{-2} + \Delta y^{-2}]^{-1/2}. \quad (12)$$

For the given cell size, the time-step sizes is about 1 fs for conventional FDTD method. Using this time-step and considering that the implicit ADI-FDTD takes five times the calculation time of the explicit FDTD in this example, the simulation will be done 20 times faster than the conventional FDTD method with a numerical dispersion accuracy of 1e-4%. In the above example, by using the ADI-FDTD method to solve both active device and electromagnetic models, the time-step can be increased again from 1 fs (Full-ADI scheme). Although this method is unconditionally stable, the time-step size that must be used to achieve the desired numerical dispersion accuracy is determined by a simple approach presented in [22]. The numerical dispersion accuracy, p , is given by

$$\sin\left(\frac{\pi}{(1-p)N}\right) = \frac{\tan(\pi s/N)}{s} \quad (13)$$

where $s = c\Delta t/\Delta_{\max}$ is the Courant number, $N = \lambda/\Delta_{\max}$ is the minimum mesh density corresponding to the maximum mesh Δ_{\max} , and c is the theoretical velocity. In the full-wave simulation, the cell size is imposed by the Debye length, which is much smaller than the practical wavelengths [12]. Thus, the CFL number ($\Delta t_{ADI-FDTD}/\Delta t_{FDTD}$) can be very large and still the numerical dispersion error of the method remains small. As (12) is a nonlinear

equation respect to the Δt , we select a proper Δt to have sufficient sample of input signal, output signals, and some harmonics of them in the time domain. Then if the calculated p from (12) for this Δt is not sufficient, a smaller Δt is tested until the value of p is acceptable. In our example the f_{\max} and Δ_{\max} are equal to 100 GHz and 1 μm , respectively. By selecting $\Delta t = 10$ fs the numerical dispersion accuracy is obtained equal to an acceptable value of 0.03% and we have 1000 samples in each period of output signals which has sufficient capability to show nonlinearity effects.

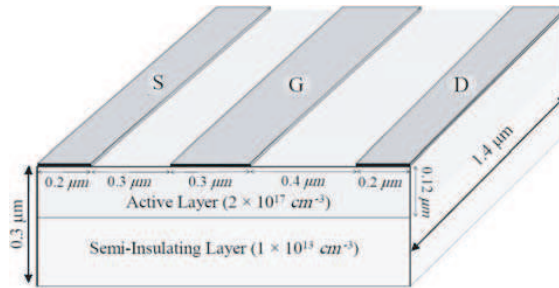


Figure 2. The simulated MESFET structure.

1) DC Simulation: The device is biased to $V_{ds} = 2\text{V}$ and $V_{gs} = -0.5\text{V}$. The state of the MESFET under dc steady state is represented by the distribution of potential and carrier density. It is to be noted that Dirichlet boundary conditions are used at the electrodes while Neumann boundary conditions are used at the other walls. As the DC simulation is not to contain the electromagnetic model, a larger time step $\Delta t = 0.1$ ps is selected for this part. Figure 3 shows the DC potential and carrier density distributions obtained using the ADI-FDTD scheme. In compare with conventional FDTD method, the CPU time for ADI-FDTD method is reduced by 83% with a maximum numerical dispersion error of 0.001%.

2) AC Simulation: To simulate the electromagnetic wave propagation, we consider the PML absorbing boundary condition. An ac excitation is applied to the gate electrode, which is given as: $V_{gs}(t) = V_{gs0} + \Delta v_{gs} \sin(\omega t)$, where V_{gs0} is the DC bias applied to the gate electrode, ω is the frequency of the applied signal, and Δv_{gs} is the peak value of the AC signal (0.1 V). Figure 4 shows the output voltages obtained by multiplying the total current by the resistance that defines the DC operating point of the transistor [23]. The output drain voltage is estimated using the ADI-FDTD method and the conventional approach. As can be seen, the results in the ADI-FDTD case and the conventional FDTD case are in good

agreement. Considering one time-step, the calculation time for the active device model is much less than the calculation time for the electromagnetic model. Therefore, there is no significant difference between calculation time of one step in the Half-ADI scheme and in the Full-ADI scheme. Therefore, the simulation until a desired time will be done approximately 200 times faster than the conventional FDTD method when Δt increases from 0.01 fs to 10 fs while the numerical dispersion error is still very small. For the simulation, $2e6$, $2e4$, and $2e3$ iterations were run with the conventional FDTD method, the half-ADI method, and the full-ADI method, respectively. The CPU time for these methods are approximately $2e6$ s, $1e5$ s, and $1e4$ s, respectively. We use a PC with a Pentium 4 processor (2.5 GHz).

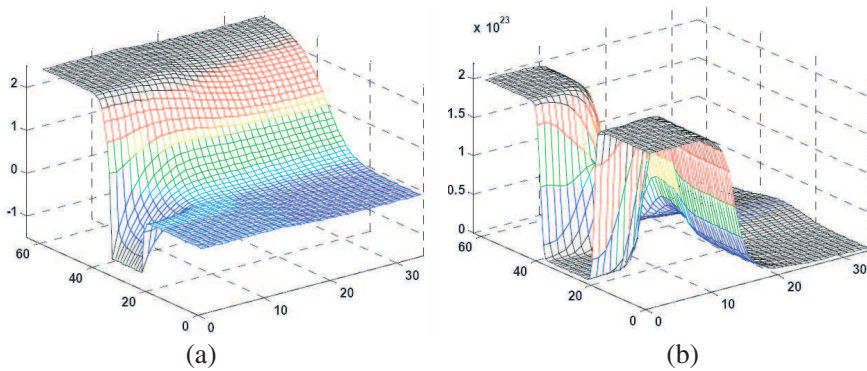


Figure 3. Sample DC results obtained using the proposed algorithm: (a) Potential distribution. (b) Carrier density distribution.

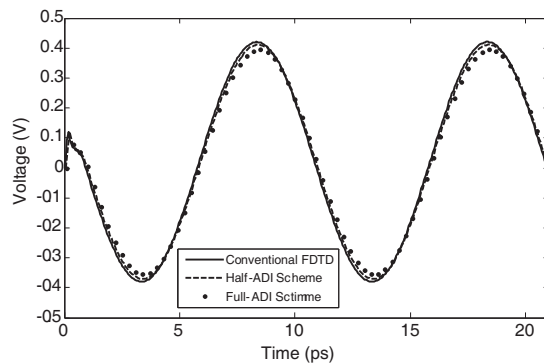


Figure 4. Output drain voltage obtained using the conventional FDTD ($\Delta t = 0.01$ fs), Half-ADI scheme ($\Delta t = 1$ fs), and Full-ADI scheme ($\Delta t = 10$ fs).

6. CONCLUSION

This work proposed a numerical method for full-wave simulation of the time dependent semiconductor devices equations in a very low calculation time in comparison with conventional methods. Using the ADI-FDTD method to solve DDM equations allows to increase the time-step size by a factor of 100 and obtaining 83% reduction in the simulation time with a negligible error. In the full-ADI scheme, we simulate the electromagnetic and active device equations simultaneously with the ADI approach. This scheme is a full implicit method and allows to increase the time-step until the numerical dispersion accuracy is acceptable. Since the size of the local minimum cell in the computational domain (which is imposed by the Debye length) is much smaller than the wavelength, the error limitation is much larger than the CFL limitation. Therefore, the ADI-FDTD method is more efficient than the conventional FDTD method for the full-wave simulation of active microwave/millimeter-wave devices. In an example, we reach over 99% reduction in the simulation time by using this approach while still have a good degree of accuracy compared to the conventional approaches.

ACKNOWLEDGMENT

This work was supported in part by Iran Telecommunication Research Center.

REFERENCES

1. Kung, F. and H. Chuah, "Modeling of bipolar junction transistor in FDTD simulation of printed circuit board," *Progress In Electromagnetics Research*, PIER 36, 179–192, 2002.
2. Afrooz, K., A. Abdipour, A. Tavakoli, and M. Movahhedi, "Time domain analysis of active transmission line using FDTD technique (application to microwave/MM-wave transistors)," *Progress In Electromagnetics Research*, PIER 77, 309–328, 2007.
3. Alsunaidi, M. A., S. M. S. Imtiaz, and S. M. El-Ghazaly, "Electromagnetic wave effects on microwave transistors using a full-wave time-domain model," *IEEE Trans. Microw. Theory Tech.*, Vol. 44, No. 6, 799–808, Jun. 1996.
4. Feng, Y. K. and A. Hintz, "Simulation of sub-micrometer GaAs MESFET's using a full dynamic transport model," *IEEE Trans. Electron Devices*, Vol. 35, 1419–1431, Sep. 1988.

5. Li, Z.-M., "Two-dimensional numerical simulation of semiconductor lasers," *Progress In Electromagnetics Research*, PIER 11, 301–344, 1995.
6. Liu, Q. H., C. Cheng, and H. Z. Massoud, "The spectral grid method: A novel fast Schrödinger-equation solver for semiconductor nanodevice simulation," *IEEE Trans. Computer-aided Design Integ. Circuit Sys.*, Vol. 23, No. 8, Aug. 2004.
7. Cheng, C., J.-H. Lee, K. H. Lim, H. Z. Massoud, and Q. H. Liu, "3D quantum transport solver based on the perfectly matched layer and spectral element methods for the simulation of semiconductor nanodevices," *Journal of Comput. Physics*, Vol. 227, No. 1, 455–471, Nov. 2007.
8. Namiki, T., "3-D ADI-FDTD method — Unconditionally stable time-domain algorithm for solving full vector Maxwell's equations," *IEEE Trans. Microw. Theory Tech.*, Vol. 48, No. 10, 1743–1748, Oct. 2000.
9. Zheng, F., Z. Chen, and J. Zhang, "Toward the development of a three-dimensional unconditionally stable finite-difference time-domain method," *IEEE Trans. Microw. Theory Tech.*, Vol. 48, No. 9, 1550–1558, Sep. 2000.
10. Kong, K. B., S. O. Park, and J. S. Kim, "Stability and numerical dispersion of 3-D Simplified sampling biorthogonal adi method," *Journal of Electromagnetic Waves and Applications*, Vol. 24, No. 1, 1–12, 2010.
11. Rouf, H. K., F. Costen, S. G. Garcia, and S. Fujino, "On the solution of 3-D Frequency dependent crank-nicolson FDTD scheme," *Journal of Electromagnetic Waves and Applications*, Vol. 23, No. 16, 2163–2175, 2009.
12. Movahhedi, M. and A. Abdipour, "Efficient numerical methods for simulation of high-frequency active devices," *IEEE Trans. Microw. Theory Tech.*, Vol. 54, No. 6, 2636–2645, Jun. 2006.
13. Cangellaris, A. C. and R. Lee, "On the accuracy of numerical wave simulations based on finite methods," *Journal of Electromagnetic Waves and Applications*, Vol. 6, No. 12, 1635–1653, 1992.
14. Castillo, S. and S. Omick, "Suppression of dispersion in FDTD solutions of Maxwell's equations," *Journal of Electromagnetic Waves and Applications*, Vol. 8, No. 9–10, 1193–1221, 1994.
15. Garcia, S. G., F. Costen, M. F. Pantojal, A. Brown, and A. R. Bretones, "Open issues in unconditionally stable schemes," *Progress In Electromagnetics Research Symposium Abstracts*, 841, Beijing, 2009.

16. Kung, F. and H. T. Chuah, "Stability of classical finite-difference time-domain (FDTD) formulation with nonlinear elements — A new perspective," *Journal of Electromagnetic Waves and Applications*, Vol. 17, No. 9, 1313–1314, 2003.
17. Liang, F. and G. Wang, "Fourth-order locally one-dimensional FDTD method," *Journal of Electromagnetic Waves and Applications*, Vol. 22, No. 14–15, 2035–2043, 2008.
18. Zhou, X. and H. Tan, "Monte Carlo formulation of field-dependent mobility for Al_xGa_{1-x}As," *Solid-State Electronics*, Vol. 38, 567–569, 1994.
19. Morton, K. W. and D. F. Mayers, *Numerical Solution of Partial Differential Equations*, 2nd Edition, University Press, New York, Cambridge, 2005.
20. Bau III, D. and L. N. Trefethen, "Numerical linear algebra," *Philadelphia: Society for Industrial and Applied Mathematics*, 1997.
21. Tomizawa, K., *Numerical Simulation of Submicron Semiconductor Devices*, Artech House, Norwood, MA, 1993.
22. Sun, G. and C. Trueman, "A simple method to determine the time-step size to achieve a desired dispersion accuracy in ADI-FDTD," *Microw. Optic. Tech. Lett.*, Vol. 40, No. 6, Mar. 2004.
23. Hussein, Y. A. and S. M. El-Ghazaly, "Extending multiresolution timedomain (MRTD) technique to the simulation of high-frequency active devices," *IEEE Trans. Microw. Theory Tech.*, Vol. 51, No. 7, 1842–1851, Jul. 2003.